Department of Signal Processing and Acoustics

Features and Applications of the Laser-induced Spark as a Monopole Source for Acoustic Impulse Response Measurements

Javier Gómez Bolaños

Aalto University

DOCTORAL DISSERTATIONS

Aalto University publication series
DOCTORAL DISSERTATIONS 98/2017

Features and Applications of the Laser-induced Spark as a Monopole Source for Acoustic Impulse Response Measurements

Javier Gómez Bolaños

A doctoral dissertation completed for the degree of Doctor of Science (Technology) to be defended, with the permission of the Aalto University School of Electrical Engineering, at a public examination held at the lecture hall AS1 of the school on 15 June 2017 at 12:00.

Aalto University
School of Electrical Engineering
Department of Signal Processing and Acoustics
Acoustics and Audio Signal Processing

Supervising professor
Professor Ville Pulkki, Aalto University, Finland

Thesis advisor
Professor Ville Pulkki, Aalto University, Finland

Preliminary examiners
Professor Ning Xiang, Rensselaer Polytechnic Institute, NY, USA
Professor Finn T. Agerkvist, Technical University of Denmark, Denmark

Opponent
Professor Angelo Farina, University of Parma, Italy

Aalto University publication series
DOCTORAL DISSERTATIONS 98/2017

ISBN 978-952-60-7447-4 (printed)
ISBN 978-952-60-7446-7 (pdf)
ISSN-L 1799-4934
ISSN 1799-4934 (printed)
ISSN 1799-4942 (pdf)
http://urn.fi/URN:ISBN:978-952-60-7446-7

Unigrafia Oy
Helsinki 2017

Finland

441 697
Printed matter

Aalto University

Aalto University, P.O. Box 11000, FI-00076 Aalto www.aalto.fi

Abstract

Author
Javier Gómez Bolaños

Name of the doctoral dissertation
Features and Applications of the Laser-induced Spark as a Monopole Source for Acoustic Impulse Response Measurements

Publisher School of Electrical Engineering

Unit Department of Signal Processing and Acoustics

Series Aalto University publication series DOCTORAL DISSERTATIONS 98/2017

Field of research Acoustics and Audio Signal Processing

Manuscript submitted 25 January 2017 **Date of the defence** 15 June 2017

Permission to publish granted (date) 27 April 2017 **Language** English

☐ **Monograph** ☒ **Article dissertation** ☐ **Essay dissertation**

Abstract
Impulse responses of acoustic systems allow us not only to analyze the acoustical behavior of the system, but also to synthesize that acoustical behavior by other means, e.g., reproducing virtual sources in rooms over headphones. Characteristics of the acoustic source like directivity, size, frequency response, and repeatability influence the accuracy of the impulse response measurement. To minimize the effect of the source in the measurements, the characteristics of the source should resemble those of an ideal acoustic point monopole, i.e., a source of infinitesimal dimensions that radiates isotropically the same sound energy in all frequency bands. Focusing a highly energetic laser pulse onto a point in space generates a pressure impulse that propagates isotropically and whose sound energy is distributed over a wide frequency range. Although laser sparks have been used extensively in ultrasound and non-linear acoustics research, its use in linear acoustics has been very limited. The work contained in this dissertation investigates the characteristics of the laser spark as a point monopole source for impulse response measurements and its use in different applications, like in scale models and small rooms. The results confirm the point monopole characteristics of the laser spark, i.e., small size, omnidirectional radiation pattern, and good repeatability. In contrast to typical sources, the laser spark allows obtaining a more accurate impulse response measurement in a frequency range that spans from few hundreds of hertz to hundreds of kilohertz. Virtual sources with controllable directivity were synthesized applying different beamforming techniques to the impulse responses measured with spatially distributed laser sparks. The synthesized source directivity was utilized in applications like directional analysis and tracking of early reflections and auralization of arbitrary source directivity.

Keywords Acoustic monopole, laser spark, impulse response measurement, beamforming, auralization

ISBN (printed) 978-952-60-7447-4 **ISBN (pdf)** 978-952-60-7446-7

ISSN-L 1799-4934 **ISSN (printed)** 1799-4934 **ISSN (pdf)** 1799-4942

Location of publisher Helsinki **Location of printing** Helsinki **Year** 2017

Pages 116 **urn** http://urn.fi/URN:ISBN:978-952-60-7446-7

Aalto-yliopisto

Aalto-yliopisto, PL 11000, 00076 Aalto www.aalto.fi

Tiivistelmä

Tekijä
Javier Gómez Bolaños

Väitöskirjan nimi
Laserilla tuotettu kipinä monopolilähteenä akustisissa impulssivastemittauksissa — ominaisuudet ja käyttötarkoitukset

Julkaisija Sähkötekniikan korkeakoulu

Yksikkö Signaalinkäsittelyn ja Akustiikan laitos

Sarja Aalto University publication series DOCTORAL DISSERTATIONS 98/2017

Tutkimusala Akustiikka ja Äänenkäsittelytekniikka

Käsikirjoituksen pvm 25.01.2017 **Väitöspäivä** 15.06.2017

Julkaisuluvan myöntämispäivä 27.04.2017 **Kieli** Englanti

☐ **Monografia** ☒ **Artikkeliväitöskirja** ☐ **Esseeväitöskirja**

Tiivistelmä
Impulssivasteen avulla voidaan analysoida miten signaali etenee lähteestä akustisen järjestelmän läpi vastaanottajalle, sekä syntetisoida tämä efekti virtuaalisena lähteenä kuulokke- tai kaiutinkuuntelussa. Akustisen lähteen ominaisuudet, kuten suuntaavuus, koko, taajuusvaste, ja herätteen toistettavuus vaikuttavat impulssivasteen mittauksen tarkkuuteen. Jotta lähteen vaikutukset minimoituisivat mittauksissa, sen tulisi vastata ideaalista akustista pistemonopolia, eli äärettömän pientä lähdettä, joka säteilee isotrooppisesti saman äänienergian kaikilla taajuuksilla. Kohdistamalla suurienerginen laserpulssi yhteen pisteeseen ilmassa voidaan luoda akustinen paineimpulssi, joka leviää isotrooppisesti, ja jonka äänienergia on jakautunut laajalle taajuusalueelle. Vaikka laserkipinöitä on käytetty laajasti ultraäänen ja epälineaarisen akustiikan tutkimuksessa, sen käyttö lineaarisessa akustiikassa on ollut erittäin vähäistä. Tämän väitöskirjan sisältämä työ tutkii laserkipinän ominaisuuksia pistemonopolina akustisen impulssivasteen mittauksessa ja sen hyödyntämistä akustiikan sovelluksissa, kuten akustisissa pienoismalleissa ja pienissä huoneissa. Tulokset todistavat että laserkipinällä on lähes ideaaliset pistemonopolin ominaisuudet, joita ovat mm. erittäin pieni lähteen koko, tasainen äänienergian säteily kaikkiin suuntiin, ja hyvä toistettavuus. Verrattuna yleisesti käytettyihin lähteisiin, laserkipinä mahdollistaa tarkemman impulssivasteen mittauksen taajuusalueella muutamasta sadasta hertsistä satoihin kilohertseihin. Työssä myös syntesoitiin virtuaalinen lähde jonka suuntakuviota voidaa hallita vapaasti. Tässä hyödynnettiin erilaisia keilanmuodostustekniikoita käytten tilassa ja ajassa hajautetuilla laserkipinöillä mitattuja tilan impulssivasteita. Syntetisoitua lähteen suuntavuutta käytettiin erilaisiin sovelluksiin, kuten varhaisten heijastuksien suunnan analyysiin ja seurantaan, sekä mielivaltaisesti suuntaavan lähteen auralisointiin.

Avainsanat Akustiinen monopolilähde, laserkipinä, impulsivastemittaus, keilanmuodostaminen, auralisaatio

ISBN (painettu) 978-952-60-7447-4 **ISBN (pdf)** 978-952-60-7446-7

ISSN-L 1799-4934 **ISSN (painettu)** 1799-4934 **ISSN (pdf)** 1799-4942

Julkaisupaikka Helsinki **Painopaikka** Helsinki **Vuosi** 2017

Sivumäärä 116 **urn** http://urn.fi/URN:ISBN:978-952-60-7446-7

Preface

This thesis is the result of the research carried out at the Department of Signal Processing and Acoustics of the School of Electrical Engineering in Aalto University, Espoo, Finland. The research contained in this thesis has received funding from the European Research Council under the European Community Seventh Framework Programme (FP7/2007-2013)*/ERC grant agreement no [240453].

First of all, I want to express my gratitude to my supervisor Prof. Ville Pulkki for the opportunity to conduct this work in his research group. I am really grateful for his trust, patience, and guidance during these years. Under Ville's supervision, I was able to research on different fields of acoustics, not only on the topic contained in this thesis, but also on audiovisuals and binaural rendering.

I would like to thank the pre-examiners Prof. Ning Xiang and Prof. Finn T. Agerkvist for their valuable comments and suggestions on the manuscript of this thesis. I also want to thank Prof. Angelo Farina for accepting to be my opponent. Special thanks to Luis Costa for helping with the language check of the thesis.

I am indebted to the co-authors of the articles contained in the thesis, Symeon Delikaris-Manias, Joona Eskelinen, Pasi Karppinen, Ilkka Huhtakallio, Dr. Cheol-Ho Jeong, and Prof. Edward Hæggström for their collaboration and hard work. It took a long time enclosed in dark rooms but we did a great job.

I want to acknowledge current and former co-workers of the acoustics lab: Akis, Alessandro, Antti, Catarina, Fabián, Henri, Henkka, Jouni, Juha, Juhani, Juho, Jukka, Julia, Julian, Jussi, Magge, Marko, Mikkis, Okko, Olli R., Olli S., Rafael, Sami, Sofoklis, Stefano, Tapani, Teemu, Tuomo, Ville S., and many others, for creating such a great work environment. It has been a privilege to work with such a great people in the

acoustics lab.

I also want to express my gratitude to my parents Ana and Juan Luis, to my brothers Oscar and Garoé, and to my life partner Lea, for their support during all these years. Finally, my special thanks to my children, Damien and Harry, who have been the milestones of my life, marking the beginning and the end of an adventure whose result is this thesis.

Espoo, May 9, 2017,

Javier Gómez Bolaños

Contents

Preface 1

Contents 3

List of Publications 5

Author's Contribution 7

List of Abbrevations 9

List of Symbols 11

1. Introduction 13

1.1 Organization of the thesis 14

2. Acoustic point monopole 15

2.1 Source strength 15

2.2 Point-like source 16

2.3 Acoustic monopole 17

2.4 Acoustic sources 18

2.4.1 Loudspeakers 18

2.4.2 Electrical spark 20

2.4.3 Other impulsive sources 21

3. Impulse response of acoustic systems 23

3.1 Measurement of impulse responses 23

3.1.1 Impulsive and continuous excitation signal 24

3.2 Effect of the source 25

3.2.1 Source response 26

3.2.2 Source directivity 26

3.3 Scale models 26

3.4 Computer simulation 27

4. Synthesis of source directivity 29

4.1 Differential array 29

4.2 Beamforming 30

4.3 Synthesis of target directivity 31

5. Laser-induced air breakdown 35

5.1 Air breakdown generation using a pulsed laser 35

5.2 Shock wave 37

5.3 Acoustic characteristics 37

6. Summary of publications 41

7. Conclusions 47

References 51

Errata 61

Publications 63

List of Publications

This thesis consists of an overview and of the following publications which are referred to in the text by their Roman numerals.

I Javier Gómez Bolaños, Pasi Karppinen, Edward Hæggström, and Ville Pulkki. An optoacoustic point source for acoustic scale model measurements. *Journal of the Acoustical Society of America Express Letters*, 133 (4), pp. EL221–EL227, April 2013.

II Javier Gómez Bolaños, Joona Eskelinen, Symeon Delikaris-Manias, Edward Hæggström, Cheol-Ho Jeong, and Ville Pulkki. Benefits and applications of laser-induced sparks in real scale model measurements. *Journal of the Acoustical Society of America Express Letters*, 138 (3), pp. EL175–EL180, September 2015.

III Javier Gómez Bolaños, Joona Eskelinen, Symeon Delikaris-Manias, Edward Hæggström, and Ville Pulkki. Laser-induced acoustic point source for accurate impulse response measurements within the audible bandwidth. *Journal of the Acoustical Society of America Express Letters*, 135 (6), pp. EL298–EL303, June 2014.

IV Joona Eskelinen, Symeon Delikaris-Manias, Javier Gómez Bolaños, Edward Hæggström, and Ville Pulkki. Beamforming with a volumetric array of massless laser spark sources – Application in reflection tracking. *Journal of the Acoustical Society of America Express Letters*, 137 (6), pp. EL389–EL395, June 2015.

V Symeon Delikaris-Manias, Javier Gómez Bolaños, Joona Eskelinen, Ilkka Huhtakallio, Edward Hæggström, and Ville Pulkki. Auralization of source radiation pattern synthesized with laser spark room responses. *Journal of the Audio Engineering Society*, 64(10), pp. 720–730, December 2015.

Author's Contribution

Publication I: "An optoacoustic point source for acoustic scale model measurements"

The present and second authors carried out a set of measurements to analyze the acoustical characteristics of the laser-induced breakdown based on the original idea of the second and fourth authors. The present author was also responsible for the analysis and wrote the paper, receiving feedback from the other authors.

Publication II: "Benefits and applications of laser-induced sparks in real scale model measurements"

The study presents the result of a cooperative work with the Technical University of Denmark, which provided a real scale model of a concert hall. The present author and the second author designed the setup and carried out the measurements for this research. The present author was responsible of the analysis of the data and wrote the article in collaboration with the second and third author. The present author edited the manuscript based on the feedback received from the other authors.

Publication III: "Laser-induced acoustic point source for accurate impulse response measurements within the audible bandwidth"

The present and the second author carried out the measurements for this research. The present author was responsible for the analysis and wrote the article in collaboration with the second and third author. The present author edited the manuscript according to the comments received from the other authors.

Publication IV: "Beamforming with a volumetric array of massless laser spark sources – Application in reflection tracking"

The present author and the first author were responsible for the measurements done in this research. The present author collaborated with the first and second author in the preparation of the manuscript, which was written and edited by the first author.

Publication V: "Auralization of source radiation pattern synthesized with laser spark room responses"

The present author collaborated with the first author in the design of the listening tests and in the preparation of the manuscript. The present and the third author were responsible for the measurements done in this research. The present author wrote part of sections 1.2 and 3.2 in the first draft of the manuscript, which was written and edited by the first author.

List of Abbrevations

BEM	boundary-element model
BRIR	binaural room impulse response
DAS	delay-and-sum
DI	directivity index
ESS	exponential sine sweep
FDTD	finite-difference time domain
FEM	finite-element model
FIR	finite impulse response
HRIR	head-related impulse response
IRS	inverse repeated sequence
LIB	laser-induced air breakdown
LSS	linear sine sweep
LTI	linear time-invariant
MIMO	multiple-in-multiple-out
MLS	maximum length sequence
Nd:YAG	neodymium-doped yttrium aluminium garnet
RIR	room impulse response
SNR	signal-to-noise ratio
TDS	time delay spectrometry
ULA	uniform linear array
WNG	white noise gain

List of Symbols

A	area on which the laser is focused
$\mathbf{A}$	array manifold
a	radius of the sphere
c	speed of sound
d	distance between elements in an array
E	energy
I_{L}	light intensity
j	imaginary unit
k	wave number, frequency bin
M	number of elements in an array
$p(t)$	sound pressure
Q	strength of the sound source
r	distance, radius
S	surface of the source
t	time
U_0	amplitude of the particle velocity normal to the surface of the source
$\vec{u}(t)$	particle velocity
$\mathbf{W}$	weights matrix
Γ	directivity of the source
$\mathbf{\Gamma}$	directivity matrix
$\mathbf{\Gamma}_{\mathrm{T}}$	target directivity matrix
Δt	pulse duration
$\delta(t)$	dirac delta function
ξ_0	amplitude of the normal surface displacement of the source

θ	azimuth angle
κ	radial direction
λ	wavelength
ρ	density of air
ϕ	elevation angle
ω	angular frequency

1. Introduction

When sound propagates inside acoustic systems, e.g., rooms, ears, or pipes, the sound is reflected, scattered, or diffracted depending on the characteristics of the boundaries set by the system. The effect of the acoustic system on the sound traveling from a source position to an observation point is known as the transfer function of the system. The transfer function of an acoustic system is assumed not to vary with time and to produce linear effects on the sound, thus making it a linear time-invariant (LTI) system. This implies that the system transfer function can be obtained by exciting the system with an impulse at the source position and measuring the response at an observation point. This measured response is known as the impulse response of the system. The use of acoustic impulse responses spans a wide range of applications, from the analysis of acoustic parameters of rooms to the rendering of virtual sources using binaural techniques.

When measuring the acoustic impulse response of a system, the sound source is typically assumed to be a point source with an omnidirectional radiation pattern that produces sufficient sound energy in the bandwidth on interest. This ensures that the acoustic system is equally excited in all directions and that the source does not influence the sound field with its presence. Therefore, the sound source is assumed to be an acoustic point monopole. Unfortunately, all these requirements cannot be achieved in practice. Loudspeakers are able to radiate sufficient sound energy over a wide frequency range, but they have finite size and a directional radiation pattern at high frequencies. On the other hand, typical impulsive sources are tiny and omnidirectional. However, they do not radiate sound efficiently at all frequencies, and the acoustic impulse may not be sufficiently repeatable.

Focusing a highly energetic laser pulse causes the breakdown of air, i.e., spark. The breakdown is characterized by a plasma ball accompanied by an acoustic impulse of large sonic energy (shock wave). The laser spark has omnidirectional sound radiation and it disappears rapidly, thus not affecting the sound field due to its presence. Therefore, this type of sound source resembles the acoustic characteristics of a point monopole. Laser-induced sparks have been used as point sources in ultrasonic research as well as in non-linear acoustics research due to their wide frequency content and large peak pressure level. Although this source does not radiate sound efficiently at very low frequencies, the produced impulse is very repeatable, thus allowing the use of signal processing methods to extend the usability to low frequencies.

The research conducted in this thesis focuses on the use of laser-induced sparks as an acoustic monopole source in linear acoustics applications. The experiments carried out in this work are mainly related to the measurement of room responses, but the results can be generalized to other acoustic systems as well. Due to the massless and omnidirectional characteristics of the spark, impulse responses of acoustic systems measured with this source are truly point-to-point responses, and so the accurate extraction of the system response from the measured impulse responses is possible. Furthermore, the point-source characteristics of the spark also simplify the combination of spatially separated responses using beamforming techniques in order to synthesize adjustable source radiation patterns that can be used to analyze specific surfaces of the system as well as to auralize more natural sound sources.

1.1 Organization of the thesis

This thesis consists of an introduction and five publications containing the author's research. The introduction is organized as follows: The monopole source and the features of typical sound sources are described in Chapter 2. Next, an overview of impulse response measurement methods, stressing the relevance of the sound source, is given in Chapter 3. Basic knowledge on beamforming techniques using monopole sources is presented in Chapter 4. The phenomena behind the laser-induced spark and its acoustical characteristics are presented in Chapter 5, followed by a summary of the publications contained in this dissertation. Finally, conclusions are addressed in Chapter 7.

2. Acoustic point monopole

If we drop a small stone into water, we can observe how a circular wave diverges from the point the stone entered the water. This is an example of how spherical waves are generated by point monopole sources. This type of source is characterized by a tiny size and omnidirectional sound emission. A common assumption in acoustic measurements is to consider the sound source to be an omnidirectional *point-like* source, thus approximating the point monopole.

In this chapter, the acoustic point monopole is briefly described, deriving the criteria for the point-like and omnidirectionality assumptions. In addition, the characteristics of typical sources are reviewed.

2.1 Source strength

Different acoustic parameters of the sound field, like pressure, particle velocity, sound intensity and acoustic power, can be obtained from the strength of the source. The strength of a sound source, Q, represents the volume of air moved by the source and is calculated for sources with finite dimensions and harmonic motion as

$$Q = \int_S \vec{u}(t) \mathrm{d}\vec{S} \,, \tag{2.1}$$

where $\vec{u}(t)= U_0 e^{j\omega t}$ is the particle velocity at each element $\mathrm{d}\vec{S}$ of the source surface S, t represents the time instant, j is the imaginary unit, and ω is the angular frequency [1]. The velocity is indeed a vector that may contain components in directions other than the normal to the surface, but in order to simplify the description of the sources given here, only the normal component of the velocity is used. The amplitude of the velocity ,U_0, is defined then as

$$U_0 = j\omega\xi_0 \,, \tag{2.2}$$

where ξ_0 is the amplitude of the displacement of the surface in the normal direction. Combining Eqs. 2.1 and 2.2, it can be deduced that a small source needs to produce a larger displacement to equal the strength of a larger source. Furthermore, an equal displacement ξ_0 at all frequencies causes the strength to vary proportionally with frequency. These characteristics of the strength explain why small sound sources have difficulty radiating low frequencies and why the size of the source is typically increased to reproduce very low frequencies so as to avoid unrealistically large displacement of the source surface.

2.2 Point-like source

A point source is an abstract entity that represents a source of infinitesimal dimensions which is defined by its strength, Q. The sound pressure $p(t)$ in a harmonic sound field of angular frequency ω at a distance r from the source can then be calculated as

$$p(r,t) = j\frac{Q\rho ck}{4\pi r}e^{j(\omega t - kr)}\Gamma(\kappa)\,, \tag{2.3}$$

where $k = \omega/c$ is the wave number, c is the speed of sound, Q is the strength of the source, and $\Gamma(\kappa)$ is the directivity of the source in the radial direction κ.

If the pressure is observed at a distance much greater than the dimensions of a real source, the sound seems to come from a point in space, and the dimensions of the source are no longer relevant to the sound field. In such cases, Eq. 2.3 can be used to estimate the pressure at the observation point. Therefore, real sources having finite size can be considered to be point-like when the sound pressure is observed in the far field ($kr \gg 1$) at a distance r greater than the dimensions of the source [1].

The source directivity $\Gamma(\kappa)$ represents how the source radiates sound energy in each direction, which may vary also with frequency. $\Gamma(\kappa)$ is a function of several factors like source dimensions and shape; number, disposition, and size of radiating surfaces; and sound wavelength λ [2]. This thesis focus on the special case where $\Gamma(\kappa) = 1$, which means that the source radiates equally in all directions (omnidirectional) and the source can be regarded as an acoustic monopole.

2.3 Acoustic monopole

The acoustic monopole source can be seen as a *pulsating* sphere, i.e., a sphere whose radius varies with time [1]. When the volume of the sphere compresses or expands, the air particles that surround the sphere move with equal radial velocity to the surface of the sphere. Since the sphere is symmetric in all radial directions, the pulsation of the sphere produces spherical waves in any homogeneous and isotropic surrounding medium [1]. The pressure $p(t)$ at a distance r from the center of the sphere of radius a can then be calculated as [1]

$$p(r,t) = j\frac{a^2 \rho c k U_0}{r} e^{j(\omega t - kr)} . \tag{2.4}$$

If the radius of a monopole is assumed to be infinitesimal ($a \to 0$), the monopole is defined only by its strength, which is known as the *point monopole* [2]. Therefore, the point monopole can be seen as a point in space from where sound is radiated omnidirectionally.

The point monopole is of great importance in acoustics. It serves as an elementary source when decomposing the wavefront following Huygen's principle, which states that each point in the wavefront can be considered as a point monopole radiating into a half space [3, 2]. Moreover, the point monopole represents the ideal source for obtaining the acoustic response of an acoustic system since it excites the system equally in all directions and it does not influence the sound field with its presence.

The acoustic monopole is also called *simple source* since it is the simplest theoretical source able to generate spherical waves [1]. A peculiarity of typical sources, like loudspeakers or pipes, is that they behave like a simple source when the maximum dimension of the source, a, is smaller than the wavelength of the produced sound ($ka \ll 1$) [1]. Therefore, to assume a sound source to be a point-like monopole, the dimensions of the source should be small enough to radiate sound omnidirectionally in the frequency band of interest without affecting the sound field, and the sound field should be observed far enough from the source ($kr \gg 1$), thus enabling the pressure to be estimated accurately using Eq. 2.4.

2.4 Acoustic sources

The characteristics of typical sources used to approximate the acoustic point monopole are described in this section.

2.4.1 Loudspeakers

Typical loudspeakers are sound sources usually with a single radiator for a specific frequency band enclosed in a rigid box. The frequency range at which loudspeakers can be regarded as monopole sources is very limited and depends strongly on the size of the loudspeaker. For a loudspeaker with maximum dimension a, the condition $ka \ll 1$ holds for very low frequencies. At higher frequencies, the loudspeaker features some directionality and cannot be regarded as a monopole. However, it can be regarded as a point-like source in many applications where the loudspeaker is placed far enough from the observation point ($kr \gg 1$). The effect of loudspeaker size can be seen in the examples of the directivity plots for two-way loudspeakers illustrated in Fig. 2.1. The smaller loud-

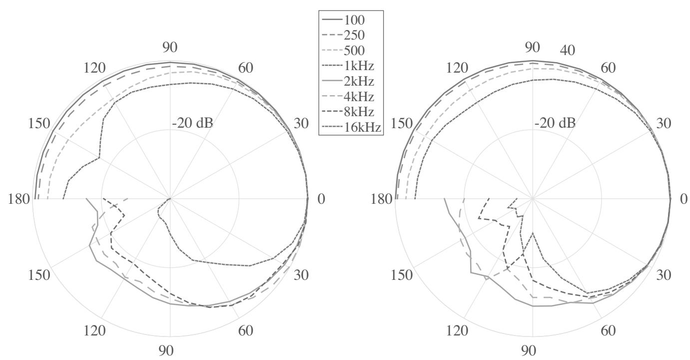

Figure 2.1. Directivity of two-way loudspeakers in the horizontal plane. (Left) Loudspeaker with a 5.1 in. woofer and a 1 in. tweeter (Tannoy Mercury V1). (Right) Loudspeaker with a 4 in. woofer and a 0.75 in. tweeter (Genelec 8020A). Symmetry in the horizontal plane is assumed. Responses are averaged in 1/6 octave bands. Frequency bands from 2 kHz to 16 kHz are presented in the lower half of the plots for clarity.

speaker (the 4 in. woofer - on the right side of Fig. 2.1) features a less directional radiation pattern at frequencies below 1 kHz than the larger loudspeaker (the 5.1 in. - on the left of Fig. 2.1). Below 250 kHz the wavelength is so large that both loudspeakers radiate omnidirectionally. The radiation pattern becomes more directional at higher frequencies where the condition $ka \ll 1$ does not hold although the radiators are also smaller.

An enclosed loudspeaker feeding the aperture of a reverse horn has been also proposed as an omnidirectional point source in [4], and improvements to this design have been presented in [5]. This type of loudspeaker improves the omnidirectional radiation pattern of typical loudspeakers but still features a directional radiation pattern at mid and high frequencies.

To improve the omnidirectional radiation of loudspeakers, several radiators emitting sound in phase can be placed in a spherical configuration using Platonic shapes. These are known as spherical loudspeakers. Among the spherical loudspeakers, the dodecahedron loudspeaker has been found to have the most omnidirectional radiation pattern [6]. However, the individual directivity of each transducer and the interaction between transducers cause a multidirectional radiation pattern at high frequencies [7]. An example of the directivity of a dodecahedron loudspeaker is given in Fig. 2.2, where the improvement in omnidirectionallity can be seen at frequencies below 1 kHz and the multidirectional radiation pattern is seen above that frequency. The omnidirectional radiation at higher frequen-

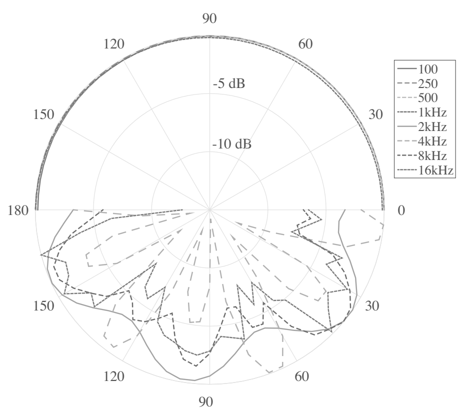

Figure 2.2. Directivity of a dodecahedron loudspeaker with $\oslash = 0.5\,\mathrm{m}$ in the horizontal plane. Symmetry in the horizontal plane is assumed. Responses are averaged in 1/6 octave bands. Frequency bands from 2 kHz to 16 kHz are presented in the lower half of the plots for clarity.

cies can be improved by reducing the size of the loudspeaker, but this decreases the strength of the source at low frequencies. An example of a micro-dodecahedron loudspeaker is given in [8].

In [9], a symmetrical three-way setup is used to design a loudspeaker with an omnidirectional radiation pattern. A ring radiator consisting of two loudspeakers with a conical enclosure facing each other has been also proposed as a better omnidirectional source than spherical loudspeakers [10]. Recently, the use of dielectric elastomer material for constructing a pulsating ball has been investigated for a hemisphere [11].

2.4.2 Electrical spark

The electrical spark is produced when a high voltage potential is applied between two electrodes that are close to each other [12, 13, 14]. This causes the electrons to jump from one electrode to the other generating a plasma line accompanied by an acoustic pulse. Electrical sparks in a small gap between electrodes ($< 5\mathrm{mm}$) produce a very repeatable and omnidirectional acoustic impulse [15]. The emitted acoustic energy is, however, weak although acceptable for certain type of applications, e.g., scale-model measurements [16]. Their small size and frequency-independent surface velocity cause sparks not to radiate sufficient sound energy at low frequencies.

To increase the acoustic energy of the spark, the electrodes must be separated with a larger gap and the electric potential has to be increased proportionally [17, 18]. Due to the larger separation of the electrodes, the spark describes a line that may follow different paths for different realizations. This has two consequences: the plasma line becomes a line radiator at audible wavelengths thus resulting in directivity [19, 15], and the waveform of the acoustic impulse may change between realizations [19] thus losing repeatability. An electrical spark device and its measured acoustic impulse and magnitude responses are illustrated in Fig. 2.3.

The acoustic impulse waveform is characterized by an abrupt pressure transient followed by a rarefaction of the medium. Due to the initial large level of the pressure pulse, the midair is over-compressed, a condition known as amplitude saturation. This causes harmonic components that extend the spectra towards ultrasound frequencies [20]. The magnitude response of this pressure signal resembles a bandpass filter centered at a frequency determined by the duration of the pulse waveform and having a 6-dB/octave decaying slope towards lower frequencies [12].

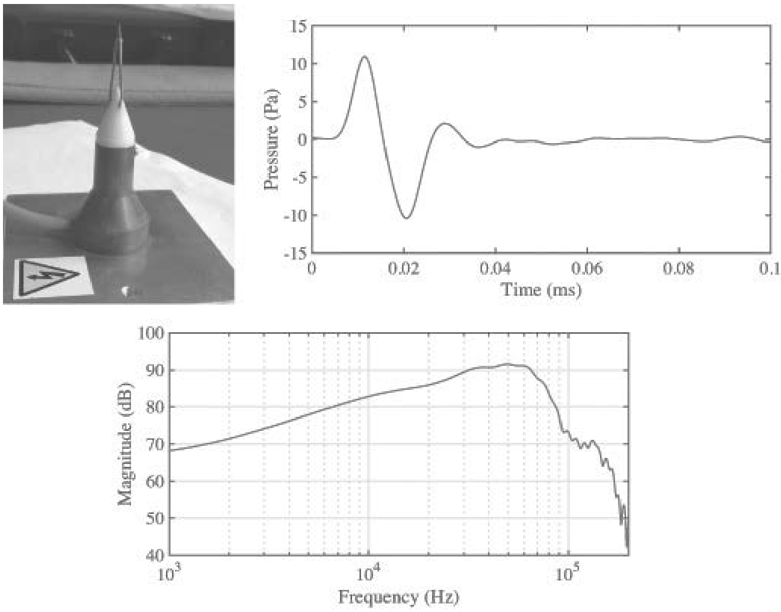

Figure 2.3. (Left) Electrical spark. (Right) The acoustic impulse produced by the electrical spark, and (bottom) the magnitude response of the acoustic impulse normalized for a 0.1 ms time window.

2.4.3 Other impulsive sources

Other impulsive sources are pistols [21], crackers [22], balloons [23], and clappers [24]. Although larger than sparks, these sources are smaller than loudspeakers, and the condition $ka \ll 1$ holds for a very wide frequency range. Thus these sources usually feature quasi-omnidirectional radiation over a very wide frequency range. Due to their greater size, these sources produce larger energy levels at lower frequencies than electrical sparks. However, these sources suffer from large variability in the produced waveform, thus having low repeatability.

Pistols, balloons, clappers, and crackers allow fast measurement of the impulse responses using portable recording devices, although, due to the lack of repeatability, these measurements are intended for fast and approximate analysis of the acoustical parameters of rooms rather than for acquiring an accurate impulse response.

3. Impulse response of acoustic systems

When an ideal acoustic impulse is generated at some point inside an acoustic system, the paths that the sound travels inside the system to a certain observation point are of different lengths, hence the reflected wavefronts arrive at the observation point at different times, producing a temporal pattern known as the impulse response of the system.

Impulse responses have been used for different applications in acoustics. Comparing the impulse reflected from a surface to the incident impulse allows the analysis of the acoustic properties of the surface [25]. The analysis of the room impulse response (RIR) permits the estimation of parameters that correlate with perceptual auditory phenomena [26, 27]. These parameters, typically known as room parameters, are used to study, design and condition auditoria like concert halls and opera houses [26]. The impulse response from a point source to the ears of a listener in free-field conditions, known as the head-related impulse response (HRIR), can be convolved with anechoic sounds to generate virtual auditory displays [28, 29]. Furthermore, the impulse response from a source inside a room to the ears of a listener, or the binaural room impulse response (BRIR), can be used for auralization [29, 30], thus permitting the perceptual analysis of the room.

This chapter describes different techniques applied to obtain the impulse response of acoustic systems. Due to the scope of this thesis, special attention is given to the effect of the sound source on the accuracy of the impulse response measurement.

3.1 Measurement of impulse responses

A practical implementation of an impulse response measurement consists of an acoustic source and a receiver placed at different positions inside the acoustic system. The measurement system is illustrated as a block diagram in Fig. 3.1.

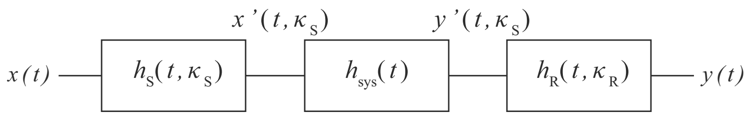

Figure 3.1. Block diagram of an acoustic impulse response measurement.

A test signal $x(t)$ is applied to a source, causing the acoustic excitation of the system. The sound field generated at the position of the source is represented by $x'(t, \kappa_{\mathrm{S}})$. The sound field at the receiver position, $y'(t, \kappa_{\mathrm{S}})$, is observed using a receiver (microphone) obtaining the signal $y(t)$. The parameter κ represents the direction-dependency (directivity) of the source, κ_{S}, or receiver, κ_{R}. Note that the direction-dependency in $x'(t, \kappa_{\mathrm{S}})$ and $y'(t, \kappa_{\mathrm{S}})$ is due to the directivity of the source and it is independent of the receiver. The measured signal $y(t)$ is then the result of the convolution of $x(t)$ with the responses of the source, $h_{\mathrm{S}}(t, \kappa_{\mathrm{S}})$; the acoustic system, $h_{\mathrm{sys}}(t)$; and the receiver, $h_{\mathrm{R}}(t, \kappa_{\mathrm{R}})$; which is expressed as

$$y(t) = x(t) \otimes h_{\mathrm{S}}(t, \kappa_{\mathrm{S}}) \otimes h_{\mathrm{sys}}(t) \otimes h_{\mathrm{R}}(t, \kappa_{\mathrm{R}})\,. \tag{3.1}$$

The response of the system, $h_{\mathrm{sys}}(t)$, does not depend on the directivity of the source and receiver, but on the position of the source and receiver inside the system, and it cannot be extracted from $y(t)$ if source and receiver are not omnidirectional. Hence the importance of the omnidirectional point source/receiver assumption. Furthermore, $h_{\mathrm{sys}}(t)$ does not change if the source and receiver are interchanged, a condition known as reciprocity [2].

3.1.1 Impulsive and continuous excitation signal

If the acoustic source generates an ideal (Dirac) impulse that propagates isotropically, then $x'(t, \kappa_{\mathrm{S}}) = \delta(t)$ and the response of the system, $h_{\mathrm{sys}}(t)$, can be directly observed at $y'(t)$. Impulsive sources attempt to emulate an ideal impulse, thus providing a fast estimate of the impulse response of the system. Due to the short duration of the impulse, reflections that arrive at the observation point close to each other are easily identifiable. However, the impulse should feature a large amplitude in order to provide sufficient sound energy at all frequencies, as stated by Parseval's theorem. This may result in non-linear effects due to amplitude saturation of the midair [31, 32, 20].

To avoid amplitude saturation, the sound energy can be distributed in time with a continuous signal, and together with signal processing techniques, the impulse response of the system can be obtained. Continuous signal methods require electro-acoustic transducers (loudspeakers) to reproduce the sound signal. The maximum length sequence (MLS) [33] and inverse repeated sequence (IRS) [34] methods use cross-correlation of a pseudo-random sequence to obtain the impulse response of the system. The linear sine sweep (LSS), typically used in time delay spectrometry (TDS) [35, 36], and the exponential sine sweep (ESS) [37] use sinusoidal signals whose frequency varies with time. The impulse response of the system is obtained after convolving the observed signal with the time-reversed excitation signal [38]. For the ESS method, a magnitude correction is also applied to compensate for the pink spectrum of the excitation signal [37, 38]. A comparison of different methods is found in [38] and [39].

3.2 Effect of the source

The effect of the source is better seen in the frequency domain, where the convolution process becomes a product of complex spectra, and Eq. 3.1 can be expressed as

$$Y(\omega) = X(\omega)H_{\mathrm{S}}(\omega, \kappa_{\mathrm{S}})H_{\mathrm{sys}}(\omega)H_{\mathrm{R}}(\omega, \kappa_{\mathrm{R}})\,. \tag{3.2}$$

To accurately extract the response of the system, $H_{\mathrm{sys}}(\omega)$, the responses of the source and receiver, $H_{\mathrm{S}}(\omega, \kappa_{\mathrm{S}})$ and $H_{\mathrm{R}}(\omega, \kappa_{\mathrm{R}})$, should be compensated. The source and receiver may be designed to have omnidirectional radiation with a flat frequency response, so that $H_{\mathrm{S}}(\omega, \kappa_{\mathrm{S}}) = H_{\mathrm{R}}(\omega, \kappa_{\mathrm{R}}) = 1$. In such a case, the block diagram illustrated in Fig. 3.1 reduces to $H_{\mathrm{sys}}(\omega)$ for these particular source and receiver positions. However, although these requirements can be obtained in practice for receivers, both requirements are difficult to achieve with acoustic sources. The response $H_{\mathrm{S}}(\omega, \kappa_{\mathrm{S}}) = 1$ is equivalent to an ideal acoustic point monopole source, which can only be approximated in practice as explained in Section 2.4. Thus the following discussion focuses then on the effect of the source, but the reasoning for receivers is equivalent.

3.2.1 Source response

If the source is omnidirectional, its response is described by $H_{\mathrm{S}}(\omega)$ for any direction. Therefore, $H_{\mathrm{S}}(\omega)$ can be compensated using the inverse source response, $H_{\mathrm{S}}^{-1}(\omega)$. This process is known as deconvolution, and it is expressed as

$$H_{\mathrm{S}}(\omega)H_{\mathrm{S}}^{-1}(\omega) = 1 \quad . \tag{3.3}$$

In practice, the inversion of the source response is done for a limited frequency range in which the signal-to-noise ratio (SNR) is sufficient. To avoid the amplification of noise at frequencies where the SNR is low, a regularization factor can be added to limit the effect of the inversion at those frequencies [40, 41].

Sometimes the source response features low SNR in the frequency band of interest, in which case averaging across several measurements improves the SNR due to the uncorrelated nature of noise. However, to make this process accurate, the response of the source should be repeatable, i.e., $H_{\mathrm{S}}(\omega)$ should not change between different measurements.

3.2.2 Source directivity

When the source features directional radiation, $H_{\mathrm{S}}(\omega, \kappa_{\mathrm{S}})$ is different in each direction. The effect of source directivity is especially relevant in enclosed spaces since the system is not excited equally in all directions. This produces an inaccurate estimation of the system response since the source response cannot be correctly removed from the measured signal using deconvolution. For instance, the non-omnidirectional radiation of the acoustic source has been found to cause inaccurate estimation of acoustical room parameters [22].

3.3 Scale models

The use of scale models to estimate the response of an acoustic system relies on the relationship between frequency, wavelength and speed of sound:

$$c = \lambda f \, . \tag{3.4}$$

To maintain a constant speed of sound, the scaling down of the dimensions of an acoustic system implies using the inverse of the scale factor on the frequency. For instance, in a 1:10 scale model, $0.1\,\mathrm{m}$ represents $1\,\mathrm{m}$ in the original system, and the analysis of the frequency band at 10 kHz is equivalent to the analysis of the 1 kHz band in the original system. The characteristics of the material used to build the scale model should match the characteristics of the original materials in order to obtain an accurate estimate of the response of the acoustic system. Furthermore, air absorption at ultrasonic frequencies does not behave in a manner proportional to the scale factor. To compensate for these differences, a different gas-medium or time-frequency processing can be applied [42, 43].

The reduced dimensions of scale models add further constraints to the characteristics of the sound source, which should be tiny in order to be considered point-like. Miniature spherical loudspeakers, as well as electrical sparks, have been usually used in scale-model measurements due to their reduced size. Some examples are found for instance in [44] and [45]. Scale models have been used to estimate the acoustic behavior of auditoria [44] or urban infrastructures [16], to analyze the acoustical properties of complex surfaces [46, 47] and to evaluate the accuracy of computer simulations [48, 49]. Auralization using binaural techniques is also achievable using scaled binaural receivers [45, 50].

3.4 Computer simulation

Computational methods can be utilized to estimate the impulse response of acoustic systems using a three-dimensional model of the system. These methods can be divided into wave-based and geometrical methods. Wave-based methods approximate the solution to the wave equation for the boundary conditions imposed by the acoustic system. These methods are the boundary-element model (BEM) [51], finite element model (FEM) [52], and finite-difference time domain (FDTD) [53].

Geometrical methods are based on the detection of the paths from the source to the receiver inside the system. These methods are mainly intended for obtaining room impulse responses [54]. The impulse response of regular enclosures can be well determined using the image-source method [55]. In this method, reflections are determined by mirroring the source with respect to the reflecting surface. The ray tracing method analyzes the propagation path of particles radiated from the source position in all directions [56]. The impulse response of the system is obtained by defining a volume around the receiver position to detect the particles that pass through. A hybrid model mixing both methods has been also proposed

[57, 58]. A comparison between geometrical methods is found in [54], and a round-robin study of different software based on these methods is found in [59].

4. Synthesis of source directivity

In Chapter 3, the acoustic point monopole was described as the optimal sound source to obtain the impulse response of an acoustic system. However, real sources, like loudspeakers or musical instruments, feature frequency-dependent directivity that may be of interest and so must be preserved in the impulse response measurement. For instance, the effect of source directivity has a great influence on the sound perceived by a listener and has clear applications in sound reproduction [60]. Therefore, to reproduce a more natural sound in auralization, efforts have been done to synthesize the directivity of sound sources [61]. Furthermore, in the field of room acoustics, the need to obtain directional information has been addressed [62] and methods for studying the acoustics of concert halls using directional sources and receivers have been proposed [63, 64, 65]. Reflection tracking methods make use of directive sources and receivers for decomposing the impulse response, which allow detailed analysis of the reflections [66].

In this chapter, a brief introduction to the synthesis of source directivity using monopole sources is given. The focus is on the synthesis of controllable directivity patterns, i.e., radiation patterns that can be steered or modified using a linear combination of monopole signals.

4.1 Differential array

A dipole is constructed by placing two monopoles with opposite phase close to each other. The dipole can be seen as the spatial derivative of the acoustic field at the dipole position. The dipole directivity is expressed as

$$\Gamma(\theta) = \cos(\theta)\,, \tag{4.1}$$

where θ represents angle with respect to the dipole axis [67]. At low frequencies, the spatial derivative of the sound field has low values, which can be compensated by using equalization of the source response or the measured signal [67].

Differential arrays are based on combining spatial derivatives of the acoustic field in order to obtain the directivity of the n^{th} order following the equation

$$\Gamma(\theta) = \sum_{i=0}^{N} a_i \cos^i(\theta)\,, \tag{4.2}$$

where N is the order, a_i are the coefficients of the spatial derivatives, and θ is the angle respect to the axis formed by the elements of the array [68].

Controlling the values of the coefficients a_i allows the adjustment of the array directivity. For instance, adjusting the coefficients a_0 and a_1 of the first order directivity ($N = 1$) permits obtaining omnidirectional directivity ($a_i = [1\,,0]$), dipole directivity ($a_i = [0\,,1]$), cardioid directivity ($a_i = [0.5\,,0.5]$), and hypercardioid directivity ($a_i = [\frac{1}{3}\,,\frac{2}{3}]$), among others [69, 70, 71].

In a three-dimensional space, first order directivity can be steered using a monopole and three orthogonal dipoles using

$$\Gamma(\theta,\phi) = a_0 + a_{10}\cos(\theta)\cos(\phi) + a_{11}\sin(\theta)\cos(\phi) + a_{12}\sin(\theta)\sin(\phi)\,, \tag{4.3}$$

where θ and ϕ are the azimuth and elevation angles, respectively, of the steering direction and a_{1j} are the first order coefficients for each orthogonal dipole j [67, 72].

Small sources feature low-efficiency radiation at low frequencies, thus having low SNR. This makes the differential array method to be most commonly used in microphone arrays.

4.2 Beamforming

Beamforming is a method by which array gain is maximized in a specific direction and reduced in others [73]. The directivity of a uniform linear array (ULA) of M elements and inter-element separation d is determined by

$$\Gamma(\theta) = \sum_{m=1}^{M} w_m^* e^{j(m-1)kd\sin(\theta)}\,, \tag{4.4}$$

where w_m contains the complex weights given to each element m of the array and $e^{j(m-1)kd\sin(\theta)}$ represents the delay at each element m of the array for a plane wave in the steering direction θ. Due to the symmetry around the line array, θ is the angle of the steering direction with respect to the axis of the array.

Equation 4.4 resembles the equation of a finite impulse response (FIR) filter, but where the delay is due to the spatial distribution of the array elements. Hence beamformers are also known as spatial filters [74]. The discretization of the spatial sampling causes adverse effects like grating lobes and spatial aliasing due to constructive and destructive interference between elements of the array. These effects can be reduced by randomizing the location of the elements of the array and by forcing the inter-element distance to comply with the Nyquist spatial sampling criterion [74].

Delay-and-sum (DAS) is a method of beamforming where w_m contains only delays [74]. The directivity of the array can then be steered by adjusting the delays given to each element of the array. The method has been typically used in public-address applications with line-loudspeaker arrays for focusing the sound radiation in different zones of the audience [75, 76, 77]. Furthermore, gain control can be introduced in w_m (shading), which reduces grating lobes [76]. In conventional beamforming, the weights w_m contain constant gain and delay for all frequencies. This affects the directivity index (DI) at low frequencies, where the phase difference between elements is small.

4.3 Synthesis of target directivity

The small DI at low frequencies can be increased by defining the beamformer in the frequency domain. Thus w_m may contain frequency-dependent gain and delay, which leads to optimal beamformers [74]. In the discrete frequency domain, the directivity of a source consisting of any array of M elements can be expressed in matrix form as

$$\mathbf{\Gamma} = \mathbf{W}^H \mathbf{A} \,, \tag{4.5}$$

where $\mathbf{\Gamma} \in \mathbb{C}^{k \times \kappa}$ are the gains at frequency bin k for each direction κ, $\mathbf{W} \in \mathbb{C}^{M \times k}$ are the weights applied to each element of the array, and $\mathbf{A} \in \mathbb{C}^{M \times \kappa}$ is the array manifold. The direction κ is function of the azimuth and elevation angles (θ, ϕ) as in Eq. 4.3.

The matrix of weights $\mathbf{W}$ can be selected such that the beamformer maintains a constant directivity across frequency, avoiding the small DI at low frequencies of conventional beamforming [78, 79]. Furthermore, $\mathbf{W}$ can be selected to reproduce a frequency-dependent arbitrary directivity like that of musical instruments [80] . To do so, $\mathbf{W}$ can be determined as a minimization problem:

$$\mathbf{W}_{\text{opt}} = \arg\min_{\mathbf{W}} \left\{ |\mathbf{\Gamma}_{\text{T}} - \mathbf{W}^H \mathbf{A}|_2^2 \right\} . \tag{4.6}$$

The least-square solution for Eq. 4.6 is given by

$$\mathbf{W}_{\text{opt}} = \mathbf{\Gamma}_{\text{T}} \mathbf{A}^{\dagger} , \tag{4.7}$$

where $\mathbf{\Gamma}_{\text{T}}$ is the target directivity and $\dagger$ represents the Moore-Penrose pseudo-inverse.

The array manifold $\mathbf{A}$ contains all the information about the array, like position, directivity, and orientation of each element of the array. For an array of identical monopole sources, $\mathbf{A}$ contains only the delays between array elements for a plane wave in the direction κ, which can be easily computed. The array manifold can be also obtained by measuring the array response [81, 82], and a method has been proposed that statistically accounts for the uncertainties in the directivity of the array elements [83]. An example of the synthesis of source directivity using this method is shown in Fig. 4.1.

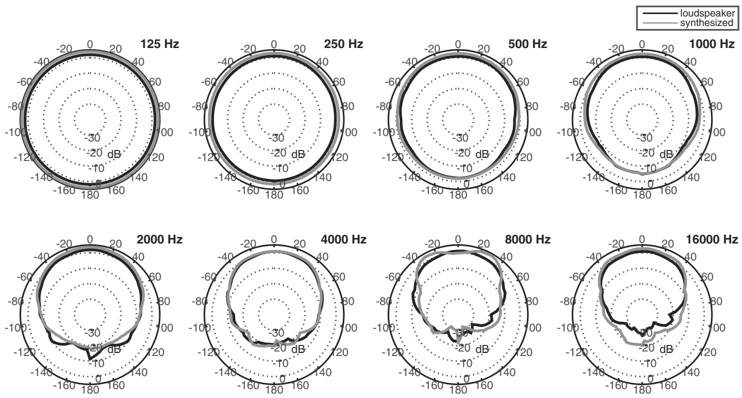

Figure 4.1. Comparison of measured and synthesized directivity using least-squares method.

A small inaccuracy in $\mathbf{A}$ may cause large errors when determining $\mathbf{W}$, especially at low frequencies where $\mathbf{W}$ acquires large values [84]. The robustness of the beamformer can be assessed by analyzing the white noise gain (WNG), i.e., the ratio of the array response in the steering direction to the total array response for spatially white noise [74]. The vector containing the WNG for each frequency bin k is determined by

$$\mathbf{WNG} = \text{diag}\left\{ (\mathbf{W}^H \mathbf{W})^{-1} \right\} \odot \text{diag}\left\{ |\mathbf{W}^H \mathbf{A}|^2 \right\} , \tag{4.8}$$

where $\text{diag}\{\cdot\}$ is the operator for extracting the diagonal of a matrix and $\odot$ is the Hadamard product.

Large values in $\mathbf{W}$ cause the WNG to decrease, thus limiting the performance of the beamformer. To reduce this effect, a regularized inverse can be applied to Eq. 4.7 using frequency-dependent approaches [85, 86] as well as singular-value-decomposition approaches [87, 88]. However, although limiting $\mathbf{W}$ improves the WNG, it consequently reduces the accuracy in the synthesis of $\mathbf{\Gamma}_{\mathrm{T}}$. Therefore, selecting the constraints for $\mathbf{W}$ is a trade-off between good performance and achieving accurate directivity synthesis [74].

The problem presented in Eq. 4.5 can be also solved using other basis functions to decompose the source directivity. Circular harmonics has been used to synthesize string instrument directivity with acoustic centering [89]. Beamforming in the spherical harmonics domain has been typically used for compact spherical arrays of loudspeakers [90, 78, 91, 92, 61, 93]. Directivity synthesis using spherical harmonics has been applied to synthesize room impulse response of directional sources [61], room reflection analysis [82], active sound control applications [94], and spatial sound reproduction [95]. To improve the limitations arising from truncating of the spherical harmonic series, the use of radiation modes has been also proposed [96, 97]. New spherical loudspeaker arrays have been designed to improve directivity synthesis by increasing the number of elements in the array [98] or by including different transducer sizes in the same array [82]. Furthermore, multiple-in-multiple-out (MIMO) systems can be realized, thus permitting directivity control at the source and receiver positions [99].

5. Laser-induced air breakdown

The use of pulsed lasers to induce pressure waves in different media has been researched for several decades. Stress waves generated by focusing a laser beam on the surface of a liquid have been used in [100] to study vaporization and thermoelastic processes. The acoustic impulse caused by the laser-induced ablation on absorbing liquids has been studied in [101]. In [102], the optimization of the laser-induced pressure-pulse generation has been investigated for transparent and opaque liquids. The propagation of acoustic waves induced by laser irradiation in solid medium has been studied in [103], [104] and [105]. The use of pulsed laser irradiation on solids as an ultrasound source has been studied in [106], where several applications were described, like non-destructive testing and acoustic imaging. Studies on gases have shown that focusing a high-energy pulsed laser can produce the breakdown of gas molecules, generating a plasma bubble or spark [107].

The research contained in this thesis focuses on the use of laser-induced sparks as monopole sources in acoustic measurements in midair. In this chapter, the phenomena behind the generation of such a spark are briefly described. The acoustical characteristics of the laser-induced spark as a monopole source are also presented.

5.1 Air breakdown generation using a pulsed laser

A laser is a device that can emit a coherent narrow beam of light. The functioning principle of lasers is based on the light amplification produced by the interaction of photons with excited atoms of a gain medium. This allows the increase of light energy in a cavity filled with a gain medium and enclosed by reflective walls, thus reflecting the light through the medium several times. This process is called optical amplification [108].

Finally, the light is released producing a light beam.

Although there are several types of laser devices, the pulsed neodymium-doped yttrium aluminium garnet (Nd:YAG) laser has been the laser device utilized in the work contained in this thesis. This type of laser uses a Nd:YAG crystal to amplify the light energy and releases the light beam using an optical switch producing a high-energy laser pulse of short duration ($< 10\,\mathrm{ns}$).

The breakdown process starts with the absorption of the light energy by the air causing an abrupt temperature rise of thousands of degrees, which generates a plasma bubble. This process is known as laser-induced air breakdown (LIB). Light intensity exceeding a threshold of $10^{15}\,\mathrm{W/m^2}$, causes air breakdown to occur. The local intensity I_L is given by

$$I_\mathrm{L} = \frac{E}{A\Delta t}\,, \tag{5.1}$$

where E is the laser pulse energy, A is the area of the laser beam at the local position, and Δt is the pulse duration. Therefore, reducing A by focusing the laser beam increases the light intensity, allowing laser beams of reduced energy to exceed the air breakdown threshold. A pulsed laser setup for air breakdown generation is presented in Fig. 5.1.

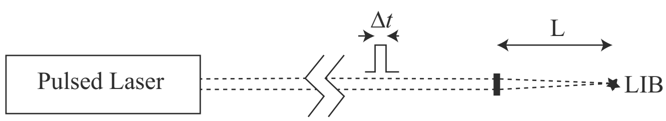

Figure 5.1. Laser-induced air breakdown setup. Δt is the pulse duration and L is the focal length of the lens.

Experiments focusing a 1064-nm laser beam of $2\,\mathrm{cm}$ diameter using a $10\,\mathrm{cm}$ focal length lens shows that incident energies larger than $16\,\mathrm{mJ}$ were sufficient to ensure air breakdown [107]. However, using a different focal length affects the laser pulse energy necessary to ensure air breakdown [109].

The plasma bubble is spherical in shape on formation, but it evolves in a direction opposite to the laser beam, forming an ellipsoidal shape, whose longer dimension is a function of the deposited energy [107, 110]. A length of approximately $5\,\mathrm{mm}$ at $90\,\mathrm{ns}$ after plasma initiation has been reported for plasma induction using a 220-mJ laser pulse [110]. After the laser pulse deceases, the temperature at the breakdown point rapidly decreases, and the plasma fades out after $100\,\mu\mathrm{s}$ for an incident energy of $150\,\mathrm{mJ}$ [111].

5.2 Shock wave

The plasma generation is accompanied by a shock wave that propagates spherically from the breakdown point with supersonic velocity [111]. The shock wave is decoupled from the plasma $1\,\mu\mathrm{s}$ after the breakdown, and its propagation velocity drops down rapidly achieving the normal speed of sound after $100\,\mu\mathrm{s}$ for an incident energy of $150\,\mathrm{mJ}$ [111]. The $100\,\mu\mathrm{s}$ time period represents a traveling distance of approximately $4\,\mathrm{cm}$ for an incident 193-nm laser beam of $135\,\mathrm{mJ}$. This distance was calculated using the velocities determined in [112].

The shock wave features a high-level pressure peak that saturates the midair, thus producing non-linear propagation of the wave [32]. The peak pressure of the acoustic impulse is a function of the deposited laser energy, and peak pressure levels up to $181\,\mathrm{dB}$ measured at $3\,\mathrm{cm}$ from the LIB have been reported [113]. Non-linear propagation of shock waves, also known as N-waves, has been studied for several decades using strong electrical sparks [19, 114, 115, 116, 117]. However, due to its smaller plasma size, larger sound pressure, and better repeatability, LIB has been proposed as a better source for studying non-linear propagation of shock waves, like those produced by blasts or sonic booms [113].

The non-linear effects are nevertheless rapidly attenuated. The distance after which one can consider linear propagation of the acoustic pulse is a function of the initial pressure level. For a peak pressure level of $181\,\mathrm{dB}$ measured at $3\,\mathrm{cm}$, distance ranges of $1.5\,\mathrm{m}$ were reported to still contain non-linear propagation effects [113]. In contrast to the conclusions in [113], results in Publication I and Publication III showed that linear propagation can be assumed at shorter distances. For instance, although the peak attenuation with distance in Publication I was found to follow similar behavior to that found in [113], the frequency response of the pulse presents linear attenuation over a wide range of the spectrum.

5.3 Acoustic characteristics

A fundamental characteristic of LIB is that it is massless, i.e., air breakdown can be induced from outside the acoustic system and the generated plasma ball rapidly disappears. For instance, the laser beam can be focused through a transparent window as in Publication I and Publication II or focused using a lens having a long focal length [109]. This avoids any influence of the source on the acoustic response of the system.

Although LIB is massless, its acoustic size is a function of the initial pressure level and, consequently, of the extension of the shock wave. As explained in Section 2.3, larger monopole sources require smaller surface displacement to generate low frequency sounds. A larger initial peak pressure level implies a larger extension of the propagating shock wave. Thus the linear acoustic impulse is seen as being caused by a larger source. Therefore, a strong LIB contains larger levels at low frequencies than a weaker LIB, which is represented by an elongation of the pulse waveform [118].

As any impulsive source, the LIB waveform consists of a short-duration impulse, resulting in a compression of the medium, followed by a rarefaction. The LIB waveform is very repeatable, as seen in Fig. 5.2 a), thus permitting the use of averaging to improve the SNR. However, repeatability of the LIB pulse can be an issue for low energy levels and long focal lengths [109]. To reduce variability in the LIB pulse with low-energy laser pulses, ablation on a small solid material has been also proposed [119].

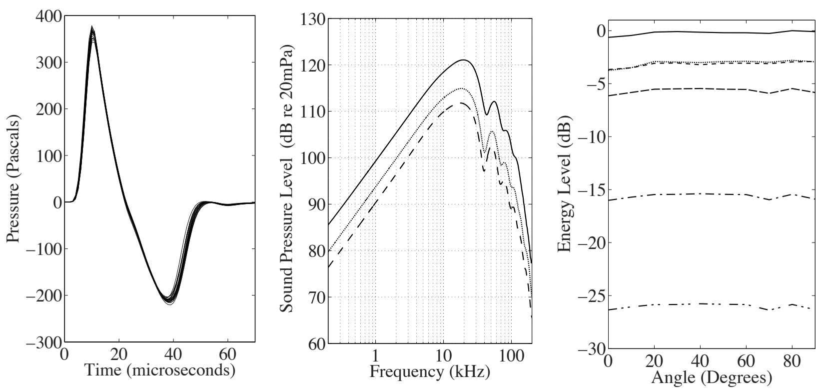

(a) (b) (c)

Figure 5.2. LIB acoustic characteristics: a) Pulse repeatability (20 pulses). b) Magnitude response at 0.423 m (solid), 0.876 m (dotted), and 1.265 m (dashed line) from the LIB. c) Pulse energy as a function of direction between $0°$ and $90°$ in octave frequency bands.

Like in the electrical spark, the magnitude response of LIB also shows a 6-dB decay towards low frequencies, nevertheless producing larger sound levels. The magnitude responses of LIB measured at three different distances are illustrated in Fig. 5.2 b). The usable acoustic spectrum spans from hundreds of Hz up to well above hundreds of kHz [113, 109]. The bandwidth can be increased by using averaging. However, the use of LIB in impulse-response measurement of very large acoustic systems, like concert halls, may be unreliable at low frequencies due to the large distances and low sound energy of LIB at those frequencies.

The small size of LIB already suggests that LIB causes omnidirectional radiation, which has been confirmed through directivity measurements in Publication I (shown in Fig. 5.2 c)), Publication III and [109].

The characteristics of LIB resemble those of an acoustic point monopole described in Section 2.3. For this reason, LIB has been proposed as a point source for accurate calibration of microphone arrays [120] and impulse-response measurements in reduced spaces [109], in addition to the research contained in this thesis.

6. Summary of publications

This section presents a summary of the contents of the publications included in this thesis.

Publication I : "An optoacoustic point source for acoustic scale model measurements"

In acoustical scale-model measurements, the size of the acoustic source is of great importance. Due to the reduced dimensions of the model, source dimensions also need to be reduced to maintain the point source assumption. Publication I presents an initial study on the reliability of LIB as an acoustic point monopole in the field of scale-model measurements. Source characteristics of LIB like repeatability, directivity, and frequency response were measured in order to confirm the monopole characteristics of LIB.

The massless character of LIB was investigated in a practical case by projecting LIB through the wall of an aquarium and measuring its impulse response. The shape of the aquarium was rectangular, and the glass walls produced very specular reflections. Thus the image-source simulation of the aquarium produces an accurate impulse response. The simulated impulse response was used to verify the point-monopole characteristics of LIB. The results (see Fig. 6.1) showed great similarity between the simulated and the measured responses, which confirms that LIB acts like an acoustic point monopole.

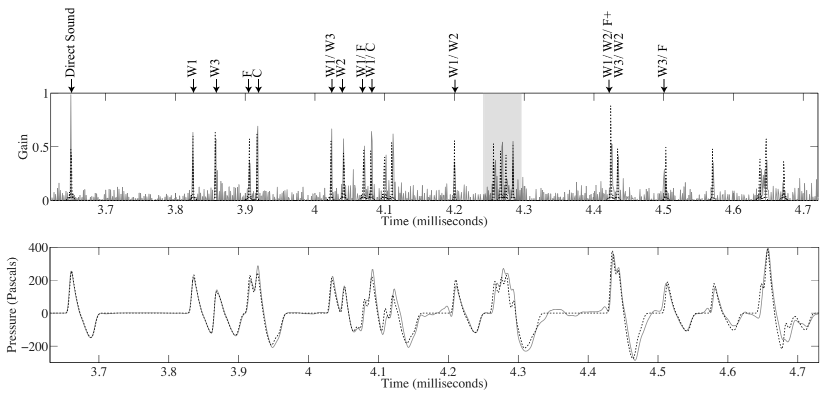

Figure 6.1. Simulated and measured impulse responses of an aquarium using LIB.

Publication II : "Benefits and applications of laser-induced sparks in real scale model measurements"

In Publication II, the benefits that LIB characteristics introduce in real scale-model measurements were investigated. A real 1:10 scale model of the Dublin National Concert Hall was modified to contain the laser setup below the stage, and the response of the model was measured using LIB, an electrical spark, and a miniature spherical loudspeaker. The LIB was projected through a glass window on the floor of the stage. Improvements in the signal level with respect to the other sources were found. The responses of LIB and the electrical spark were extracted accurately from the measured responses using deconvolution, but not for the spherical loudspeaker due to its directional behavior at high frequencies. The massless characteristic of LIB arose as an important feature, since it allows shifting of the LIB without modifying the acoustic system. This is not possible with the other sources because they feature a finite volume that must be moved inside the model. Shifting the LIB between consecutive measurements allows off-line combination of monopole sources into orthogonal dipoles and averaged monopole signals. These signal were combined to produce cardioid source directivity that was steered in order to scan the model. The scanning was used to identify the origin of the first reflections that arrive at the receiver, as depicted in Fig. 6.2.

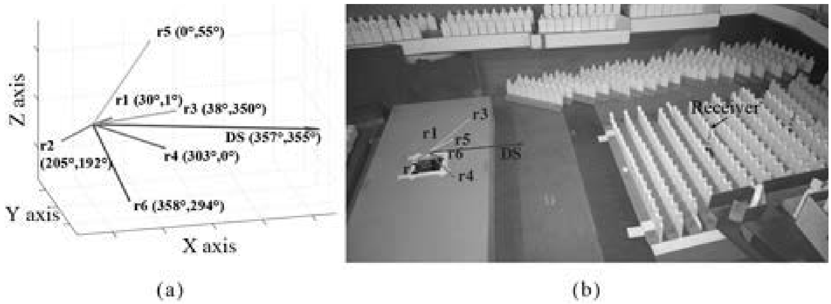

Figure 6.2. Identification of the direction of the reflective surfaces that cause the first reflections arriving at the receiver by scanning the scale model using a combination of spatially distributed LIBs.

Publication III : "Laser-induced acoustic point source for accurate impulse response measurements within the audible bandwidth"

The research in Publication III investigates the characteristics of LIB that were studied in Publication I and Publication II, but focuses now on the audible bandwidth. The laser setup was installed inside a listening room and a series of measurements were carried out to assess repeatability, frequency response, linear propagation, and directivity within the audible frequency range. The results show that LIB is very repeatable, and thus averaging can be used to improve the poor SNR at low frequencies. The improvement in SNR allows the use of deconvolution down to 100 Hz, so covering a large portion of the audible bandwidth.

The room impulse response was measured with LIB, a spherical loudspeaker, and a directional loudspeaker. Removing the source response using deconvolution shows that LIB produces a more accurate response, where reflections are clearly separated, not attenuated due to source directivity, and source shadowing is avoided (see Fig. 6.3).

Publication IV : "Beamforming with a volumetric array of massless laser spark sources – Application in reflection tracking"

A typical application of directional sources in room-impulse-response measurements is to scan the room in order to track the origin of reflections. This allows us to identify and study the reflective surfaces separately. Publication IV investigates the use of a volumetric array of LIB in reflection tracking applications.

Due to the high time resolution and monopole nature of the LIB pulses, an array of LIBs is ideal for applying DAS beamforming to the room im-

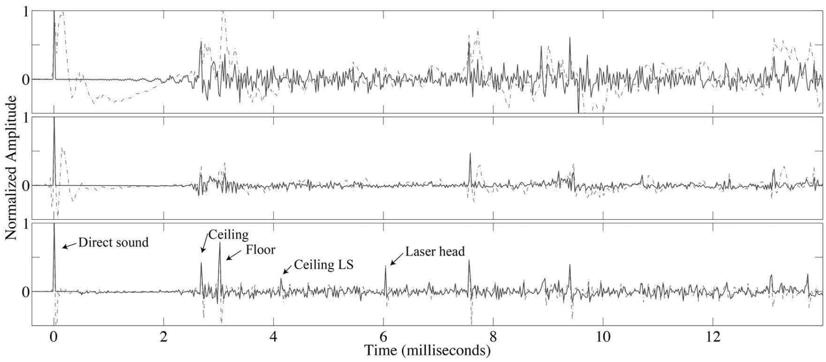

Figure 6.3. Measured (dash line) and deconvolved (solid line) room impulse responses using a spherical loudspeaker (top box), a directional loudspeaker (center box), and LIB (bottom box).

pulse responses measured with the LIB array. The performance of the beamformer was analyzed for the original LIB and for the deconvolved responses, showing that the DI improves when deconvolution is applied to the measured responses. The reflection tracking capabilities of the LIB array were demonstrated by scanning the beam in the horizontal and vertical planes to identify the reflections produced inside the room.

Publication V : "Auralization of source radiation pattern synthesized with laser spark room responses"

The auditory impression of a source in a room can be elicited to a listener through auralization. However, typical auralization methods are based on convolving anechoic source sounds with room responses obtained from measurements of sources with incorrect directivity, or from computer simulations where major characteristics of the room are not accurately represented. Publication V explores the idea of providing an accurate response of the real room where the source directivity can be controlled. A framework for controlled auralization of directional sources in real rooms is proposed and evaluated. The framework is illustrated in Fig. 6.4. The point-to-point response of the room for a set of source positions (source array) can be combined using optimal beamforming techniques to match any target source directivity. The resulting responses can then be used for auralization using the preferred reproduction method.

The method presented in Fig. 6.4 was evaluated by measuring a room using a volumetric array of LIBs. A least-squares optimization was utilized to determine the beamforming filters for the array. Synthesized

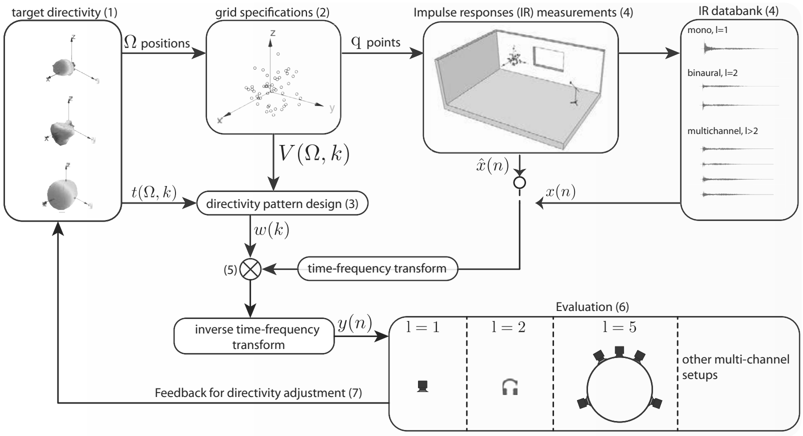

Figure 6.4. Framework for auralization of directional sources in real rooms.

and original responses were compared, showing great similarity between them. The results of formal listening tests showed that the proposed method produces a close auditory impression to a reference auralization of the target source.

7. Conclusions

The characteristics of the LIB resembles those of a theoretical point monopole: a source of infinitesimal dimensions and omnidirectional radiation that is fully characterized by its strength. Due to its high energy, tiny dimensions, wide frequency content, and short duration, LIB has been used in different fields of research, like non-linear acoustics and ultrasounds. This thesis presents a study of LIB as an acoustic point source in the field of linear acoustics, especially for the measurement of the impulse response of acoustic systems in midair.

Measurements in acoustic scale models requires that sound sources have small dimensions, omnidirectional radiation, and sufficient sound energy content in the scaled frequency range. The suitability of LIB as an acoustic source for scale-model measurements is investigated in Publication I and Publication II. Publication I shows that LIB not only fulfills the source requirements, but also avoids any effects due to the presence of the source inside the model. The capability to externally generate the acoustic excitation of the enclosed space is indeed a unique characteristic of LIB. Hence, LIB is regarded as being massless. In Publication I, the measured response of a model using LIB was compared to its computer simulation assuming a point monopole source. The results are in excellent agreement, thus confirming the monopole characteristics of LIB in a reduced scale. The benefits that LIB can provide in comparison to typical sources was investigated in Publication II, thus extending the research in Publication I. A scale model of a concert hall was measured using LIB, an electrical spark, and a miniature spherical loudspeaker, and a comparison between the responses showed the better performance of LIB. The greatest benefit, nevertheless, was the massless characteristic of LIB that allowed the generation of an off-line array of monopole sources without affecting the acoustic system. This permitted the synthesis of a controllable directional pattern used to identify the origin of early reflections.

A more challenging application is the use of LIB within the audible bandwidth. Due to the 6-dB decay towards low frequencies in the magnitude response, measurements using LIB suffer from low SNR at those frequencies. Publication III investigates the reliability of LIB measurements in the audible bandwidth. The high repeatability of LIB permits the use of averaging to improve the SNR, and so enables the use of deconvolution to accurately remove the source response from a measured room response. The room response using LIB was found to be more accurate than using a spherical loudspeaker and a directional loudspeaker since directional and shadowing effects were avoided.

The point monopole characteristics of LIB were exploited in Publication IV and Publication V to synthesize off-line controllable source directivity using a volumetric array of LIB. Similarly to Publication II, in Publication IV, the origin of reflections were identified by scanning a synthesized source directivity. In this case, however, the DAS method was applied, showing the suitability of LIB for such an application. Publication V presents the use of a volumetric LIB array and the least-square beamforming method to synthesize arbitrary source directivity in auralization applications. The advantage of using LIB relies on the accuracy of the measured room response, showed in Publication III, and in the simplicity of using closely spaced monopole sources in the beamforming process. Although beamformers using closely spaced array elements suffer from low DI at low frequencies, natural sound sources also have low DI at these frequencies, which permits accurate synthesis of the directivity.

The reduced SNR at low frequencies discourages the use of LIB in large spaces if low frequencies are of interest due to the large distances to the receiver position. Also the large averaging may extend the duration of the measurement in excess. Since spherical loudspeakers behave as monopoles at low frequencies, a combination of the two acoustic sources may provide an accurate measurement of large spaces at all frequencies. Furthermore, independently driven spherical loudspeakers can be used to synthesize controllable directivity, thus encouraging the combination of spherical loudspeakers and an array of LIB for synthesizing arbitrary source directivity.

The use of double beamforming using MIMO systems, i.e., beamforming at the source and receiver positions, can be also applicable, which is very attractive as an auralization method for real rooms. Such a method enables the synthesis of arbitrary source directivity and arbitrary receiver directivity inside the room. For instance, the sound of musical instruments inside the room could be binaurally reproduced using individual HRIRs of different listeners but the same set of measured room impulse responses.

This work shows that LIB has some advantageous properties for acoustical measurements, however, the use of high-energy lasers rises big concerns related to safety and usability. The use of high-energy lasers is indeed dangerous outside controlled environments, and laser beams that have been reflected several times can contain hazardous energy levels, especially for the eyes. Moreover, adjusting the focusing lens and the laser device requires time, and it should be repeated if the setup is placed in a new position, thus reducing the usability. To solve these concerns, future research topics can be outlined here. A further possibility to develop the system would be to enclose the laser beam in an optic fiber with integrated focusing lens. This improves the usability and safety since the LIB can be placed freely without readjustment of the setup and also the laser beam would not propagate in the air. Furthermore, ablation on a small solid object can be produced instead of LIB to avoid the propagation of the laser beam after the focusing lens. Finally, if the LIB or ablation is enveloped by an acoustically transparent material that stops light without affecting the acoustic pulse, safety issues could be completely solved as the light emitted by the laser would not propagate to the environment.

References

[1] L. E. Kinsler and A. R. Frey, *Fundamentals of Acoustics*. John Willey & Sons, 1950.

[2] F. Fahy, *Foundations of Engineering Acoustics*. Academic Press, 2001.

[3] E. Skudrzyk, *The Foundations of Acoustics*. Springer-Verlag, 1971.

[4] J.-D. Polack, L. S. Christensen, and P. M. Juhl, "An innovative design for omnidirectional sound sources," *Acta Acustica united with Acustica*, vol. 87, no. 4, pp. 505–512, 2001.

[5] S. Ortiz, B. Kolbrek, P. Cobo, L. M. González, and C. de la Colina, "Point source loudspeaker design: Advances on the inverse horn approach," *Journal of the Audio Engineering Society*, vol. 62, no. 5, pp. 345–354, 2014.

[6] C. Quested, A. Moorhouse, B. Piper, and B. Hu, "An analytical model for a dodecahedron loudspeaker applied to the design of omni-directional loudspeaker arrays," *Applied Acoustics*, vol. 85, pp. 161–171, 2014.

[7] T. W. Leishman, S. Rollins, and H. M. Smith, "An experimental evaluation of regular polyhedron loudspeakers as omnidirectional sources of sound," *The Journal of the Acoustical Society of America*, vol. 120, no. 3, pp. 1411–1422, 2006.

[8] S. Hosoe, T. Nishino, K. Itou, and K. Takeda, "Development of micro-dodecahedral loudspeaker for measuring head-related transfer functions in the proximal region," in *Proceedings of the IEEE International Conference on Acoustics, Speech, and Signal Processing, ICASSP*, pp. 329–332, 2006.

[9] P. Valtchev, D. Dimitrov, and R. Artarski, "Spherical sound source for acoustic measurements," in *Proceedings of the Audio Engineering Society Convention 133*, Oct 2012.

[10] R. Kruse, A. Häußler, and S. van de Par, "An omnidirectional loudspeaker based on a ring-radiator," *Applied Acoustics*, vol. 74, no. 12, pp. 1374–1377, 2013.

[11] N. Hosoya, S. Baba, and S. Maeda, "Hemispherical breathing mode speaker using a dielectric elastomer actuator," *The Journal of the Acoustical Society of America*, vol. 138, no. 4, pp. EL424–EL428, 2015.

[12] R. E. Klinkowstein, “A study of acoustic radiation from an electrical spark discharge in air,” Master’s thesis, Massachusetts Institute of Technology, 1974.

[13] R. Wyber, “The design of a spark discharge acoustic impulse generator,” *IEEE Transactions on Acoustics, Speech, and Signal Processing*, vol. 23, pp. 157–162, Apr 1975.

[14] R. C. Cabot, O. K. McDaniel, and H. E. Breed, “Acoustic impulse generation by high energy spark dischargers,” in *Proceedings of the Audio Engineering Society Convention 58*, Nov 1977.

[15] C. Ayrault, P. Béquine, and S. Baudin, “Characteristics of a spark discharge as an adjustable acoustic source for scale model measurements,” in *Proceedings of the Acoustics 2012, Nantes*, April 2012.

[16] J. Picaut and L. Simon, “A scale model experiment for the study of sound propagation in urban areas,” *Applied Acoustics*, vol. 62, no. 3, pp. 327–340, 2001.

[17] D. F. Farson, H. W. Choi, and S. I. Rokhlin, “Electrical discharges between platinum nanoprobe tips and gold films at nanometre gap lengths,” *Nanotechnology*, vol. 17, no. 1, p. 132, 2006.

[18] C. Ayrault, P. Béquine, and L. Mathieu, “Experimental study of a spark discharge as an acoustic source,” in *Proceedings of the Intenational Congress on Acoustics, ICA 2007, Madrid*, September 2007.

[19] W. M. Wright and N. W. Medendorp, “Acoustic radiation from a finite line source with N-Wave excitation,” *The Journal of the Acoustical Society of America*, vol. 43, no. 5, pp. 966–971, 1968.

[20] A. J. Campanella, “Finite amplitude distortion of spherically diverging intense sound waves in air,” *The Journal of the Acoustical Society of America*, vol. 67, no. 1, pp. 6–14, 1980.

[21] M. Lamothe and J. Bradley, “Acoustical characteristics of guns as impulse sources,” *Canadian Acoustics*, vol. 13, no. 2, 1985.

[22] R. San Martín, M. Arana, J. Machín, and A. Arregui, “Impulse source versus dodecahedral loudspeaker for measuring parameters derived from the impulse response in room acoustics,” *The Journal of the Acoustical Society of America*, vol. 134, no. 1, pp. 275–284, 2013.

[23] J. Pätynen, B. F. Katz, and T. Lokki, “Investigations on the balloon as an impulse source,” *The Journal of the Acoustical Society of America*, vol. 129, no. 1, pp. EL27–EL33, 2011.

[24] D. Sumarac-Pavlovic, M. Mijic, and H. Kurtovic, “A simple impulse sound source for measurements in room acoustics,” *Applied Acoustics*, vol. 69, no. 4, pp. 378–383, 2008.

[25] C. Nocke, “In-situ acoustic impedance measurement using a free-field transfer function method,” *Applied Acoustics*, vol. 59, no. 3, pp. 253–264, 2000.

[26] A. C. Gade, *Acoustics in Halls for Speech and Music*, ch. 9, pp. 344–377. Springer, 2007.

[27] ISO 3382-1, “Acoustics. Measurement of room acoustic parameters.Part 1: Performance spaces,” Standard 3382-1:2009, International Standard Organization, Geneva, Switzerland, 2009.

[28] F. L. Wightman and D. J. Kistler, “Headphone simulation of free-field listening. I: Stimulus synthesis,” *The Journal of the Acoustical Society of America*, vol. 85, no. 2, pp. 868–878, 1989.

[29] H. Møller, “Fundamentals of binaural technology,” *Applied Acoustics*, vol. 36, no. December 1991, pp. 171–218, 1992.

[30] M. Kleiner, B.-I. Dalenbäck, and P. Svensson, “Auralization—an overview,” *Journal of the Audio Engineering Society*, vol. 41, no. 11, pp. 861–875, 1993.

[31] D. T. Blackstock, “Connection between the Fay and Fubini solutions for plane sound waves of finite amplitude,” *The Journal of the Acoustical Society of America*, vol. 39, no. 6, pp. 1019–1026, 1966.

[32] D. A. Webster and D. T. Blackstock, “Finite-amplitude saturation of plane sound waves in air,” *The Journal of the Acoustical Society of America*, vol. 62, no. 3, pp. 518–523, 1977.

[33] D. D. Rife and J. Vanderkooy, “Transfer-function measurement with maximum-length sequences,” *Journal of the Audio Engineering Society*, vol. 37, no. 6, pp. 419–444, 1989.

[34] C. Dunn and M. J. Hawksford, “Distortion immunity of MLS-derived impulse response measurements,” *Journal of the Audio Engineering Society*, vol. 41, no. 5, pp. 314–335, 1993.

[35] R. C. Heyser, “Acoustical measurements by time delay spectrometry,” *Journal of the Audio Engineering Society*, vol. 15, no. 4, pp. 370–382, 1967.

[36] M. A. Poletti, “Linearly swept frequency measurements, time-delay spectrometry, and the Wigner distribution,” *Journal of the Audio Engineering Society*, vol. 36, no. 6, pp. 457–468, 1988.

[37] A. Farina, “Simultaneous measurement of impulse response and distortion with a swept-sine technique,” in *Proceedings of the Audio Engineering Society Convention 108*, Feb 2000.

[38] S. Müller and P. Massarani, “Transfer-function measurement with sweeps,” *Journal of the Audio Engineering Society*, vol. 49, no. 6, pp. 443–471, 2001.

[39] G.-B. Stan, J.-J. Embrechts, and D. Archambeau, “Comparison of different impulse response measurement techniques,” *Journal of the Audio Engineering Society.*, vol. 50, no. 4, pp. 249–262, 2002.

[40] B. Hunt, “Deconvolution of linear systems by constrained regression and its relationship to the wiener theory,” *IEEE Transactions on Automatic Control*, vol. 17, pp. 703–705, Oct 1972.

[41] O. Kirkeby and P. A. Nelson, "Digital filter design for inversion problems in sound reproduction," *Journal of the Audio Engineering Society*, vol. 47, no. 7/8, pp. 583–595, 1999.

[42] J. D. Polack, A. H. Marshall, and G. Dodd, "Digital evaluation of the acoustics of small models: The midas package," *The Journal of the Acoustical Society of America*, vol. 85, no. 1, pp. 185–193, 1989.

[43] J.-D. Polack, X. Meynial, and V. Grillon, "Auralization in scale models: Processing of impulse response," *Journal of the Audio Engineering Society*, vol. 41, no. 11, pp. 939–945, 1993.

[44] P. S. Veneklasen, "Model techniques in architectural acoustics," *The Journal of the Acoustical Society of America*, vol. 47, no. 2A, pp. 419–423, 1970.

[45] N. Xiang and J. Blauert, "Binaural scale modelling for auralisation and prediction of acoustics in auditoria," *Applied Acoustics*, vol. 38, no. 2, pp. 267–290, 1993.

[46] M. Almgren, "Acoustic boundary layer influence on scale model simulation of sound propagation: Experimental verification," *Journal of Sound and Vibration*, vol. 110, no. 2, pp. 247–259, 1986.

[47] J. K. Ryu and J. Y. Jeon, "Subjective and objective evaluations of a scattered sound field in a scale model opera house," *The Journal of the Acoustical Society of America*, vol. 124, no. 3, pp. 1538–1549, 2008.

[48] P. Luizard, M. Otani, J. Botts, L. Savioja, and B. F. Katz, "Comparison of sound field measurements and predictions in coupled volumes between numerical methods and scale model measurements," *Proceedings of Meetings on Acoustics*, vol. 19, no. 1, 2013.

[49] M. Cairoli, E. Moretti, and A. Gade, "New opera house in Astana: A recent opportunity to use a room acoustic scale model," *The Journal of the Acoustical Society of America*, vol. 133, no. 5, pp. 3581–3581, 2013.

[50] P. Robinson and N. Xiang, "Design, construction, and evaluation of a 1:8 scale model binaural manikin," *The Journal of the Acoustical Society of America*, vol. 133, no. 3, pp. EL162–EL167, 2013.

[51] S. M. Kirkup, *The boundary element method in acoustics*. Integrated sound software, 2007.

[52] L. L. Thompson, "A review of finite-element methods for time-harmonic acoustics," *The Journal of the Acoustical Society of America*, vol. 119, no. 3, pp. 1315–1330, 2006.

[53] P. Mokhtari, H. Takemoto, R. Nishimura, and H. Kato, "Computer simulation of HRTFs for personalization of 3D audio," *Proceedings of the 2nd International Symposium on Universal Communications, ISUC 2008*, pp. 435–440, 2008.

[54] J. H. Rindel, "The use of computer modeling in room acoustics," *Journal of vibroengineering*, vol. 3, no. 4, pp. 41–72, 2000.

[55] J. B. Allen and D. A. Berkley, "Image method for efficiently simulating small-room acoustics," *The Journal of the Acoustical Society of America*, vol. 65, no. 4, pp. 943–950, 1979.

[56] A. Krokstad, S. Strom, and S. Sørsdal, "Calculating the acoustical room response by the use of a ray tracing technique," *Journal of Sound and Vibration*, vol. 8, no. 1, pp. 118–125, 1968.

[57] M. Vorländer, "Simulation of the transient and steady-state sound propagation in rooms using a new combined ray-tracing/image-source algorithm," *The Journal of the Acoustical Society of America*, vol. 86, no. 1, pp. 172–178, 1989.

[58] G. M. Naylor, "ODEON—Another hybrid room acoustical model," *Applied Acoustics*, vol. 38, no. 2-4, pp. 131–143, 1993.

[59] I. Bork, "A Comparison of Room Simulation Software—The 2nd Round Robin on Room Acoustical Computer Simulation," *Acta Acustica united with Acustica*, vol. 86, no. 6, pp. 943–956, 2000.

[60] F. E. Toole, *Sound Reproduction: Loudspeakers and Rooms*. Taylor & Francis, 2012.

[61] M. Pollow, P. Dietrich, M. Kunkemöller, and M. Vorländer, "Synthesis of room impulse responses for arbitrary source directivities using spherical harmonic decomposition," in *Proceedings of the IEEE Workshop on Applications of Signal Processing to Audio and Acoustics, WASPAA*, pp. 301–304, Oct 2011.

[62] J. Bradley, "Review of objective room acoustics measures and future needs," *Applied Acoustics*, vol. 72, no. 10, pp. 713–720, 2011.

[63] S. Tervo, J. Pätynen, and T. Lokki, "Acoustic reflection path tracing using a highly directional loudspeaker," in *Proceedings of the IEEE Workshop on Applications of Signal Processing to Audio and Acoustics, WASPAA*, pp. 245–248, Oct 2009.

[64] J. Pätynen, S. Tervo, and T. Lokki, "A loudspeaker orchestra for concert hall studies," in *Proceedings of the The Seventh International Conference On Auditorium Acoustics*, pp. 45–52, 2009.

[65] J. Pätynen, S. Tervo, and T. Lokki, "Analysis of concert hall acoustics via visualizations of time-frequency and spatiotemporal responses," *The Journal of the Acoustical Society of America*, vol. 133, no. 2, pp. 842–857, 2013.

[66] S. Tervo, J. Pätynen, and T. Lokki, "Acoustic reflection localization from room impulse responses," *Acta Acustica united with Acustica*, vol. 98, no. 3, pp. 418–440, 2012.

[67] J. Eargle, "Chapter 5—First-order directional microphones," in *The Microphone Book (Second Edition)* (J. Eargle, ed.), pp. 66–90, Oxford: Focal Press, second edition ed., 2004.

[68] E. D. Sena, H. Hacihabiboglu, and Z. Cvetkovic, "On the design and implementation of higher order differential microphones," *IEEE Transactions on Audio, Speech, and Language Processing*, vol. 20, pp. 162–174, Jan 2012.

[69] G. W. Elko and A.-T. N. Pong, "A simple adaptive first-order differential microphone," in *Proceedings of the IEEE Workshop on Applications of Signal Processing to Audio and Acoustics, WASPAA*, pp. 169–172, Oct 1995.

[70] G. W. Elko, "Microphone array systems for hands-free telecommunication," *Speech Communication*, vol. 20, no. 3, pp. 229–240, 1996.

[71] H. Teutsch and G. W. Elko, "First-and second-order adaptive differential microphone arrays," in *Proceecings of the International Workshop on Acoustic Echo and Noise Control, IWAENC*, pp. 35–38, 2001.

[72] G. W. Elko and A.-T. N. Pong, "A steerable and variable first-order differential microphone array," in *Proceedings of the IEEE International Conference on Acoustics, Speech, and Signal Processing, ICASSP*, pp. 223–226, Apr 1997.

[73] B. D. Van Veen and K. M. Buckley, "Beamforming: A versatile approach to spatial filtering," *IEEE Audio, Speech, and Signal Processing, ASSP magazine*, vol. 5, no. 2, pp. 4–24, 1988.

[74] M. R. Bai, J.-G. Ih, and J. Benesty, *Acoustic Array Systems: Theory, Implementation, and Application*. John Wiley & Sons, 2013.

[75] D. L. Klepper and D. W. Steele, "Constant directional characteristics from a line source array," in *Proceedings of the Audio Engineering Society Convention 14*, Oct 1962.

[76] D. G. Meyer, "Multiple-beam, electronically steered line-source arrays for sound-reinforcement applications," *Journal of the Audio Engineering Society*, vol. 38, no. 4, pp. 237–249, 1990.

[77] D. B. D. Keele Jr., "Implementation of straight-line and flat-panel constant beamwidth transducer (CBT) loudspeaker arrays using signal delays," in *Proceedings of the Audio Engineering Society Convention 113*, Oct 2002.

[78] L. C. Parra, "Steerable frequency-invariant beamforming for arbitrary arrays," *The Journal of the Acoustical Society of America*, vol. 119, no. 6, pp. 3839–3847, 2006.

[79] M. M. Boone, W.-H. Cho, and J.-G. Ih, "Design of a highly directional endfire loudspeaker array," *Journal of the Audio Engineering Society*, vol. 57, no. 5, pp. 309–325, 2009.

[80] O. Warusfel, P. Derogis, and R. Causse, "Radiation synthesis with digitally controlled loudspeakers," in *Proceedings of the Audio Engineering Society Convention 103*, 1997.

[81] M. Kolundzija, C. Faller, and M. Vetterli, "Baffled circular loudspeaker array with broadband high directivity," in *Proceedings of the IEEE International Conference on Acoustics, Speech, and Signal Processing, ICASSP*, pp. 73–76, 2010.

[82] M. Pollow, J. Klein, P. Dietrich, G. K. Behler, and M. Vorländer, "Optimized spherical sound source for room reflection analysis," in *Proceecings of the International Workshop on Acoustic Echo and Noise Control, IWAENC*, pp. 1–4, 2012.

[83] L. Bianchi, R. Magalotti, F. Antonacci, A. Sarti, and S. Tubaro, "Robust beamforming under uncertainties in the loudspeakers directivity pattern.," in *Proceedings of the IEEE International Conference on Acoustics, Speech, and Signal Processing, ICASSP*, pp. 4448–4452, 2014.

[84] E. Mabande and W. Kellermann, “Towards superdirective beamforming with loudspeaker arrays,” in *International Congress on Acoustics*, 2007.

[85] O. Kirkeby, P. A. Nelson, H. Hamada, and F. Orduna-Bustamante, “Fast deconvolution of multichannel systems using regularization,” *IEEE Transactions on Speech and Audio Processing*, vol. 6, no. 2, pp. 189–194, 1998.

[86] A. Farina, A. Capra, L. Chiesi, and L. Scopece, “A spherical microphone array for synthesizing virtual directive microphones in live broadcasting and in post production,” in *Proceedings of the Audio Engineering Society Conference: 40th International Conference: Spatial Audio: Sense the Sound of Space*, 2010.

[87] F. M. Fazi and P. A. Nelson, “The ill-conditioning problem in sound field reconstruction,” in *Proceedings of the Audio Engineering Society Convention 123*, 2007.

[88] P.-A. Gauthier, C. Camier, Y. Pasco, A. Berry, E. Chambatte, R. Lapointe, and M.-A. Delalay, “Beamforming regularization matrix and inverse problems applied to sound field measurement and extrapolation using microphone array,” *Journal of Sound and Vibration*, vol. 330, no. 24, pp. 5852–5877, 2011.

[89] N. R. Shabtai, G. Behler, and M. Vorländer, “Generation of a reference radiation pattern of string instruments using automatic excitation and acoustic centering,” *The Journal of the Acoustical Society of America*, vol. 138, no. 5, pp. EL480–EL486, 2015.

[90] P. Kassakian and D. Wessel, “Characterization of spherical loudspeaker arrays,” in *Proceedings of the Audio Engineering Society Convention 117*, Oct 2004.

[91] F. Zotter, A. Sontacchi, and R. Holdrich, “Modeling a spherical loudspeaker system as multipole source,” *Fortschritte der Akustik*, vol. 33, no. 1, p. 221, 2007.

[92] J. Atkins, “Robust beamforming and steering of arbitrary beam patterns using spherical arrays,” in *Proceedings of the IEEE Workshop on Applications of Signal Processing to Audio and Acoustics, WASPAA*, pp. 237–240, Oct 2011.

[93] B. Rafaely and D. Khaykin, “Optimal model-based beamforming and independent steering for spherical loudspeaker arrays,” *IEEE Transactions on Audio, Speech, and Language Processing*, vol. 19, pp. 2234–2238, Sept 2011.

[94] B. Rafaely, “Spherical loudspeaker array for local active control of sound,” *The Journal of the Acoustical Society of America*, vol. 125, no. 5, pp. 3006–3017, 2009.

[95] M. A. Poletti, T. Betlehem, and T. D. Abhayapala, “Higher-order loudspeakers and active compensation for improved 2d sound field reproduction in rooms,” *Journal of the Audio Engineering Society*, vol. 63, no. 1/2, pp. 31–45, 2015.

[96] A. M. Pasqual, J. R. De França Arruda, and P. Herzog, "Application of acoustic radiation modes in the directivity control by a spherical loudspeaker array," *Acta Acustica united with Acustica*, vol. 96, no. 1, pp. 32–42, 2010.

[97] A. M. Pasqual and V. Martin, "On the acoustic radiation modes of compact regular polyhedral arrays of independent loudspeakers.," *The Journal of the Acoustical Society of America*, vol. 130, no. 3, pp. 1325–1336, 2011.

[98] R. Avizienis, A. Freed, P. Kassakian, and D. Wessel, "A compact 120 independent element spherical loudspeaker array with programable radiation patterns," in *Proceedings of the Audio Engineering Society Convention 120*, May 2006.

[99] H. Morgenstern and B. Rafaely, "Spherical loudspeaker array beamforming in enclosed sound fields by MIMO optimization," in *Proceedings of the IEEE International Conference on Acoustics, Speech, and Signal Processing, ICASSP*, pp. 370–374, May 2013.

[100] M. W. Sigrist and F. K. Kneubühl, "Laser-generated stress waves in liquids," *The Journal of the Acoustical Society of America*, vol. 64, no. 6, pp. 1652–1663, 1978.

[101] D. Kim, M. Ye, and C. Grigoropoulos, "Pulsed laser-induced ablation of absorbing liquids and acoustic-transient generation," *Applied Physics*, vol. 67, no. 2, pp. 169–181, 1998.

[102] H. Tran Van, J.-L. Augé and, and P. Rain, "Study of the generation of the pressure pulse in the laser induced pressure pulse method: Optimization of the process," in *10th IEEE International Conference on Solid Dielectrics, ICSD*, pp. 1–4, july 2010.

[103] R. J. Dewhurst, D. A. Hutchins, S. B. Palmer, and C. B. Scruby, "Quantitative measurements of laser-generated acoustic waveforms," *Journal of Applied Physics*, vol. 53, no. 6, pp. 4064–4071, 1982.

[104] L. R. F. Rose, "Point-source representation for laser-generated ultrasound," *The Journal of the Acoustical Society of America*, vol. 75, no. 3, pp. 723–732, 1984.

[105] D. H. Hurley and J. B. Spicer, "Point-source representation for laser-generated ultrasound in an elastic, transversely isotropic half-space," *Journal of Applied Physics*, vol. 86, no. 6, pp. 3423–3427, 1999.

[106] S. J. Davies, C. Edwards, G. S. Taylor, and S. B. Palmer, "Laser-generated ultrasound: its properties, mechanisms and multifarious applications," *Journal of Physics D: Applied Physics*, vol. 26, no. 3, p. 329, 1993.

[107] Y.-L. Chen, J. Lewis, and C. Parigger, "Spatial and temporal profiles of pulsed laser-induced air plasma emissions," *Journal of Quantitative Spectroscopy and Radiative Transfer*, vol. 67, no. 2, pp. 91–103, 2000.

[108] A. E. Siegman, *Lasers*. University Science Books, 1986.

[109] N. Hosoya, M. Nagata, and I. Kajiwara, "Acoustic testing in a very small space based on a point sound source generated by laser-induced breakdown: Stabilization of plasma formation," *Journal of Sound and Vibration*, vol. 332, no. 19, pp. 4572–4583, 2013.

[110] C. Bindhu, S. Harilal, M. Tillack, F. Najmabadi, and A. Gaeris, "Energy absorption and propagation in laser-created sparks," *Applied Spectroscopy*, vol. 58, pp. 719–726, 2004.

[111] H. Sobral, M. Villagrán-Muniz, R. Navarro-González, and A. Raga, "Temporal evolution of the shock wave and hot core air in laser induced plasma," *Applied Physics Letters*, vol. 77, pp. 3158–3160, 2000.

[112] M. Thiyagarajan and J. E. Scharer, "Experimental investigation of 193-nm laser breakdown in air," *IEEE Transactions on Plasma Science*, vol. 36, pp. 2512–2521, Oct 2008.

[113] Q. Qin and K. Attenborough, "Characteristics and application of laser-generated acoustic shock waves in air," *Applied Acoustics*, vol. 65, no. 4, pp. 325–340, 2004.

[114] W. M. Wright, "Propagation in air of N-waves produced by sparks," *The Journal of the Acoustical Society of America*, vol. 73, no. 6, pp. 1948–1955, 1983.

[115] A. Loeb, M. Loebenstein, A. Ludmirsky, S. Eliezer, S. Maman, and Y. Gazit, "Point explosion simulation by fast spark discharges," *Journal of Applied Physics*, vol. 57, no. 7, pp. 2501–2506, 1985.

[116] P. Yuldashev, M. Averiyanov, V. Khokhlova, S. Ollivier, and P. Blanc-Benon, "Nonlinear spherically divergent shock waves propagating in a relaxing medium," *Acoustical Physics*, vol. 54, pp. 32–41, 2008.

[117] P. Yuldashev, S. Ollivier, M. Averiyanov, O. Sapozhnikov, V. Khokhlova, and P. Blanc-Benon, "Nonlinear propagation of spark-generated N-waves in air: Modeling and measurements using acoustical and optical methods," *The Journal of the Acoustical Society of America*, vol. 128, no. 6, pp. 3321–3333, 2010.

[118] E. Manikanta, L. V. Kumar, P. Venkateshwarlu, C. Leela, and P. P. Kiran, "Effect of pulse duration on the acoustic frequency emissions during the laser-induced breakdown of atmospheric air," *Applied Optics*, vol. 55, pp. 548–555, Jan 2016.

[119] N. Hosoya, I. Kajiwara, T. Inoue, and K. Umenai, "Non-contact acoustic tests based on nanosecond laser ablation: Generation of a pulse sound source with a small amplitude," *Journal of Sound and Vibration*, vol. 333, no. 18, pp. 4254–4264, 2014.

[120] C. J. Bahr, N. S. Zawodny, B. Bertolucci, J. Li, M. Sheplak, and L. N. Cattafesta, "A plasma-based non-intrusive point source for acoustic beamforming applications," *Journal of Sound and Vibration*, vol. 344, pp. 59–80, 2015.

Errata

Publication I

In this publication the term laser-induced pressure pulse (LIPP) is used to name laser-induced breakdown (LIB). To maintain accordance with following publications LIPP should be substituted with LIB.

Aalto-DD 98/2017

ISBN 978-952-60-7447-4 (printed)
ISBN 978-952-60-7446-7 (pdf)
ISSN-L 1799-4934
ISSN 1799-4934 (printed)
ISSN 1799-4942 (pdf)

Aalto University
School of Electrical Engineering
Department of Signal Processing and Acoustics
www.aalto.fi

BUSINESS +
ECONOMY

ART +
DESIGN +
ARCHITECTURE

SCIENCE +
TECHNOLOGY

CROSSOVER

DOCTORAL
DISSERTATIONS